Sixth International Conference on Durability of Concrete Structures **Paper Number TIM06**
18 - 20 July 2018
University of Leeds, Leeds, West Yorkshire, LS2 9JT, United Kingdom

Influence of Pore Structure on Relative Chloride Diffusion Coefficient in Unsaturated Cementitious Materials

Y. Zhang and G. Ye
Faculty of Civil Engineering and Geosciences, Delft University of Technology, Delft, The Netherlands

ABSTRACT

Chloride-induced corrosion of reinforcement in concrete structures is a serious issue in engineering practice. This paper investigates the influence of pore structure on the relative chloride diffusion coefficient D_{rc} in unsaturated cementitious materials. The effects of various pore features, including porosity, pore size, and pore connectivity, on the continuity of water-filled pores in unsaturated porous systems are analyzed based on the Kelvin law and water desorption process. In the experimental program, different cementitious materials (OPC, slag, fly ash, and limestone powder) were used to prepare paste and mortar samples. The D_{rc} of the mortar samples (one year old) at various degrees of water saturation was determined based on the Nernst-Einstein equation and conductivity tests. The pore structure of the paste samples (one year old) was measured by the mercury porosimetry technique. It is found that a finer pore size distribution or lower pore connectivity tends to result in a lower D_{rc}. The pore size effect on the D_{rc} is pronounced primarily at high saturation levels. The D_{rc} at low saturation levels is dominated by the pore connectivity effect. The mortars blended with fly ash or slag exhibit lower D_{rc}-value than the OPC mortar of the same saturation level.

Keywords: Durability, Chloride diffusion, Water saturation, Pore structure, Cementitious materials

1.0 INTRODUCTION

Chloride-induced reinforcement corrosion is a major durability problem in marine concrete structures. The chloride diffusion coefficient is widely used to describe the capacity of concrete to resist chloride penetration. Previous studies on this subject were mostly based on chloride penetration tests of saturated concretes (Patel *et al*. 2016). Marine concretes, however, are seldom saturated. The knowledge about the chloride diffusion in unsaturated concretes is a prerequisite for accurate durability design of reinforced concrete structures.

In saturated concrete the connected pores are all available for ionic diffusion. In unsaturated concrete the connected pores can be divided into three parts. The first part of the connected pores is filled with gas that impedes the ionic diffusion. The second part refers to those pores that remain filled with water, but cannot form a continuous path for ionic diffusion. The third part refers to the continuous water-filled pores that allow for ionic diffusion. The continuity of water-filled pores in unsaturated porous systems depends not only on the degree of water saturation, but also on the pore structure.

Relative chloride diffusion coefficient D_{rc}, a ratio of chloride diffusion coefficient at unsaturated state over that at saturated state, has often been adopted to describe the chloride diffusion in unsaturated pore systems. The D_{rc} can vary significantly for different cementitious materials, because of the changes in the pore structure and associated changes of the continuity of water-filled pores.

This work is to study the influence of pore structure on the continuity of water-filled pores and hence on the D_{rc} in unsaturated cementitious materials. The effect of the pore structure on the continuity of water-filled pores is analyzed based on the Kelvin-law and water desorption in porous systems. In parallel, experiments are carried out. The pore structure of cementitious materials is measured by the mercury porosimetry technique. The D_{rc} of cementitious materials is determined based on the Nernst-Einstein equation and conductivity measurements.

2.0 WATER CONTINUITY IN UNSATURATED PORE SYSTEMS

2.1 Definition of Water Continuity

Water continuity η_w defines the continuity of water-filled pores in a porous system. It is expressed as: $\eta_w=N_w/N_{Sat}$, where N_w and N_{Sat} represent the number of channels available for ionic transport in the porous system at a particular degree of water saturation S_w and at saturated state, respectively. For a given S_w, a higher water continuity η_w leads to a higher relative chloride diffusion coefficient D_{rc}.

Whether a channel is available for ionic transport depends on the moisture state in the pores. Figure 1

shows three typical moisture states in a pore in view of water desorption process.

a) Initially, the pore is fully water-filled (Fig. 1a).
b) In a desorption process, water loss starts from the central part of the pore and the gas phase gradually fills the pore. The pore becomes partially water-filled (Fig. 1b).
c) The pore is considered drained if only an adsorbed water film is present (Fig. 1c). The thickness t of the water film depends on the relative humidity in the pore system.

Ionic transport is possible in fully or partially water-filled pores, but is not possible in a drained pore. A channel is not available for ionic transport if one drained pore is present in the channel.

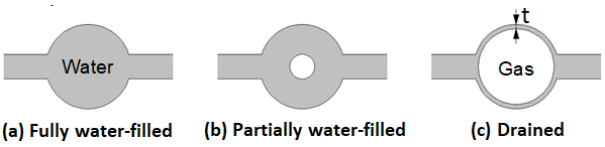

Fig. 1. Change of moisture state in a pore with water desorption process. The pore is considered drained if only a thin water film (thickness t) is present

In saturated pore systems, $N_w=N_{Sat}$ and $\eta_w=1$. With decreasing degree of water saturation S_w, the number of drained pores is increased, resulting in smaller N_w and hence lower η_w. When the S_w is below a critical level, the remaining water-filled pores cannot form a connected path for ionic transport, i.e. $N_w=0$ and $\eta_w=0$. For a given S_w, the η_w may differ for different pore systems. As shown below, the effects of various pore features on water continuity η_w will be analyzed based on the Kelvin law and water desorption process.

2.2 Effect of Pore Structure on Water Continuity

Porosity Effect on Water Continuity (Same Pore Size Distribution and Same Pore Connectivity)

Figure 2 shows the water desorption in two porous systems (I and II) with varying porosities (but with same pore size distribution and pore connectivity). System I has one channel ($N_{Sat}(I)=1$, porosity ϕ_I). System II has two channels ($N_{Sat}(II)=2$, porosity $\phi_{II}=2\phi_I$). Each channel consists of small pores (diameter d_1) and large pores (diameter d_2).

a) At saturated state ($S_w=100\%$), $N_w(I)=1$ and $N_w(II)=2$; $\eta_w(I)=1/1=1$ and $\eta_w(II)=2/2=1$.
b) At the same saturation level ($S_w=70\%$), the large pores d_2 in both systems I and II are drained, i.e. $N_w(I)=N_w(II)=0$ and $\eta_w(I)=\eta_w(II)=0$.

It is found that for the same pore size distribution and same pore connectivity, the porous systems with varying porosities exhibit the same relationship between water continuity η_w and saturation level S_w.

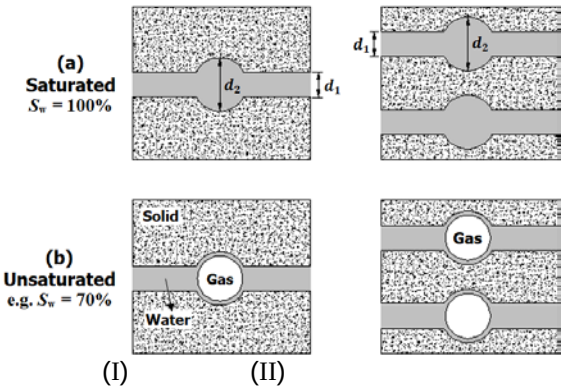

Fig. 2. Two porous systems (I and II) with varying porosities ($\phi_{II}=2\phi_I$) exhibiting the same water continuity with the same degree of water saturation, S_w

Pore Size Effect on Water Continuity (Same Porosity)

Figure 3 shows the water desorption in two porous systems (I and II) with varying pore sizes. System I has one channel ($N_{Sat}(I)=1$) consisting of large pores (diameter D_1) and small pores (diameter D_2). System II has two channels ($N_{Sat}(II)=2$) consisting of pores with diameters $d_1=D_1/2$, $d_2=\sqrt{3}D_1/2$, $d_3=D_2/2$, and $d_4=\sqrt{3}D_2/2$. Systems I and II have the same porosity (i.e. $D_1^2=d_1^2+d_2^2$ and $D_2^2=d_3^2+d_4^2$), but they are different in the pore size distribution.

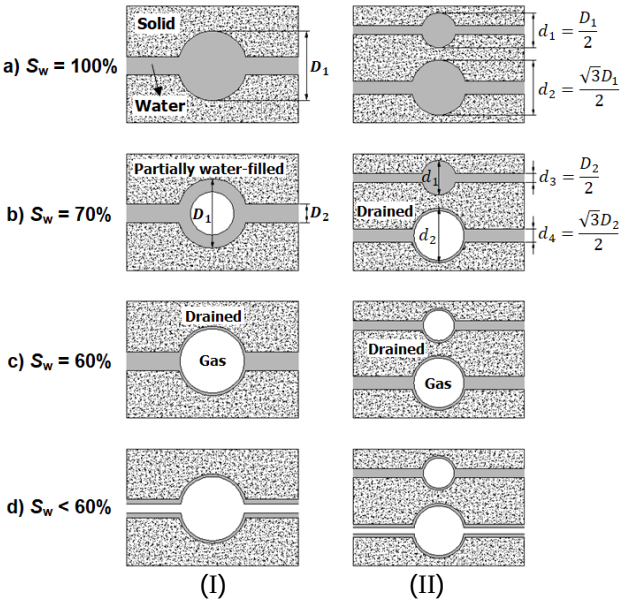

Fig. 3. Schematic representation of water desorption in two porous systems (I and II) with varying pore sizes. The finer pores are easier to be drained.

a) At $S_w=100\%$, $\eta_w(I)=1/1=1$ and $\eta_w(II)=2/2=1$.
b) With decrease of saturation level, i.e. $S_w=70\%$, the pores d_2 in system II are drained, i.e. $N_w(II)=1$ and $\eta_w(II)=1/2$. In contrast, the pores D_1 in system I remain partially water-filled allowing ionic transport, i.e. $N_w(I)=1$ and $\eta_w(I)=1$.

c) At S_w=60%, the pores D_1 in system I become drained, and the pores d_1 and d_2 in system II are also drained. Ionic transport is not possible in both systems I and II, i.e. $\eta_w(I)=\eta_w(II)=0$.
d) At S_w<60%, it holds: $\eta_w(I)=\eta_w(II)=0$. Further loss of water no longer alters the water continuity in both systems I and II.

It is found that for a given water saturation S_w the water continuity η_w tends to be lower in the porous system with a finer pore size distribution. The pore size effect on water continuity η_w is pronounced at high S_w levels, but becomes weak at low S_w levels.

Pore Connectivity Effect on Water Continuity

In unsaturated porous systems, the water phase accumulates preferentially in the small pores while the gas phase tends to fill the large pores (Kelvin law). The ability of the (water-filled) small pores to form a continuous path for ionic transport is influenced by their connectivity with the (gas-filled) large pores. Figure 4 shows two porous systems I and II. Both consist of small pores (diameter d_1) and large pores (diameter d_2), but they have different pore connectivities. The water desorption process leads to different water continuities in the two systems.

- In system I, the small pores d_1 are highly interconnected and they have no connection with the large pores d_2. The water-filled small pores d_1 are easy to form continuous paths for ionic transport when the water loss occurs in the large pores d_2.
- In system II, the small pores d_1 are not interconnected. Instead, they are connected through the large pores d_2. In case of water loss in the large pores d_2, the water-filled small pores d_1 are difficult to form a continuous path for ionic transport.

It is found that higher pore connectivity (Fig. 4-I) tends to result in higher water continuity η_w in unsaturated porous systems.

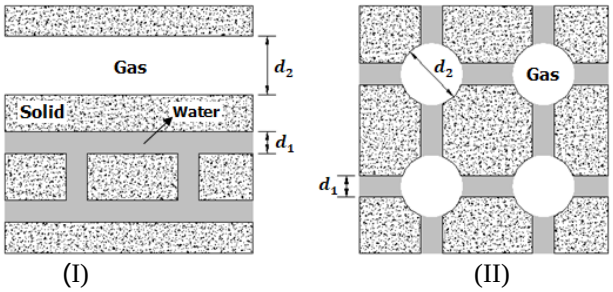

Fig. 4. Water desorption in two porous systems (I and II), where the connections between small pores (diameter d_1) and large pores (diameter d_2) are different.

In case of water loss in the large pores d_2, highly interconnected small pores (system I) are easy to form continuous water-filled paths, while poorly connected small pores (system II) are difficult to form a continuous water-filled path.

Whether the small pores are interconnected (Fig. 4-I) or they are connected through the large pores (Fig. 4-II) can be examined from the ink-bottle effect measured by mercury porosimetry technique. High pore connectivity corresponds to weak ink-bottle effect (Fig. 4-I), while low pore connectivity corresponds to severe ink-bottle effect (Fig. 4-II).

3.0 EXPERIMENTAL PROGRAM

3.1 Materials and Samples

Paste and mortar samples were prepared. The one-year-old paste samples were used for pore structure measurements. The one-year-old mortar samples were first preconditioned to uniform water saturation ranging from 18 to 100%, and then conducted with conductivity tests. To obtain uniform water saturation, each mortar sample (50 mm thick) was oven-dried at 50 ˚C to get a preassigned loss of water, followed with a moisture redistribution procedure to ensure a homogenous moisture distribution. More details about the sample preconditioning procedures can be referred to a previous work (Zhang and Ye, 2018).

The raw materials used were ordinary Portland cement (OPC, CEM I 42.5N) and supplementary cementitious materials, i.e. fly ash (FA), ground granulated blast furnace slag (BFS), and limestone powder (LP). The mixture proportions of the binders are shown in Table 1.

Table 1. Mixture proportions for the binders

Binders	Raw materials and replacement by weight				w/b ratio
	OPC	FA	BFS	LP	
P5	100%	-	-	-	0.5
PF5	70%	30%	-	-	0.5
PB5	30%	-	70%	-	0.5
PFL5	65%	30%	-	5%	0.5

3.2 Pore Structure Measurement

The water-filled pores that contribute to the ionic transport in unsaturated porous systems are usually small in size. Characterization of the small capillary pores becomes a necessity. For pore structure analysis of cementitious materials, the mercury intrusion porosimetry (MIP) technique is widely used. Due to the ink-bottle effect, the 1st intrusion of MIP is considered inappropriate to identify the real pore size distribution (Diamond 2000). The 2nd intrusion, however, has little ink-bottle effect and provides a more truthful size distribution of the small capillary pores in cement paste (Ye 2003). Figure 5 shows an example of the cumulative intrusion volume with applied pressure in the 1st and 2nd intrusion-extrusion cycles.

The pore size distribution of paste samples was determined from the 2nd intrusion of MIP and using

the Washburn equation (Washburn 1921). The average pore diameter d_a, accounting for the fineness of pore size in porous systems, is expressed as (Aligizaki 2006):

$$d_a = \frac{4V_t}{S_t} \quad (1)$$

where V_t [m^3/m^3] and S_t [m^2/m^3] are the total pore volume and total pore surface area, respectively.
The pore connectivity η_p of each paste sample was deduced from the MIP test, and expressed as the quotient of the effective porosity ϕ_e over the total porosity ϕ_t (Garboczi 1990).

$$\eta_p = \frac{\phi_e}{\phi_t} \times 100\% \quad (2)$$

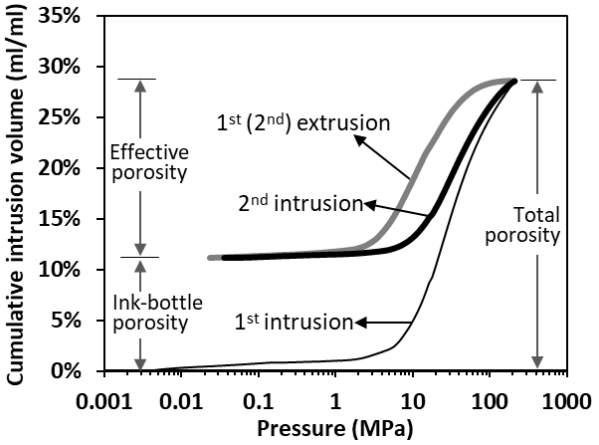

Fig. 5. Cumulative intrusion volume of OPC paste (w/b=0.5, 28-day-old) obtained from MIP in the 1st and 2nd intrusion-extrusion cycles

3.3 Conductivity Measurement

The chloride diffusion coefficient can be determined from the conductivity measurement. The Nernst-Einstein equation (Eq. (3)) gives that the ratio of conductivity σ_p of the pore solution to conductivity σ [S/m] of the cementitious material is equal to the ratio of chloride diffusion coefficient D_p in the pore solution to chloride diffusion coefficient D [m^2/s] in the cementitious material.

$$\frac{\sigma_p}{\sigma} = \frac{D_p}{D} \quad (3)$$

The D_p-value is around 1.5×10^{-9} m^2/s at room temperature when the chloride concentration is within 0.1~1.0 mol/L. From Eq. (3), the relative chloride diffusion coefficient D_{rc} can be deduced:

$$D_{rc} = \frac{D_{S_w}}{D_{Sat}} = \frac{\sigma_{S_w}}{\sigma_{Sat}} \cdot \frac{\sigma_{p,Sat}}{\sigma_{p,S_w}} \quad (4)$$

where D_{S_w} and D_{Sat} are the chloride diffusion coefficient of the cementitious material at a particular degree of water saturation and at saturated state, respectively. σ_{Sat} and $\sigma_{p,Sat}$ are the conductivity at saturated state for the cementitious material and the pore solution, respectively. σ_{S_w} and σ_{p,S_w} are the conductivity at a particular degree of water saturation for the cementitious material and the pore solution, respectively.

The values of the parameters (σ_{Sat}, σ_{S_w}, $\sigma_{p,Sat}$, and σ_{p,S_w}) were derived based on conductivity tests. The details can be referred to a previous work (Zhang and Ye, 2018). The relative chloride diffusion coefficient D_{rc} was subsequently described as a function of the degree of water saturation S_w.

4.0 EXPERIMENTAL RESULTS AND DISCUSSION

4.1 Pore Size Distribution

Figure 6 shows the pore size distribution (PSD) of different pastes obtained from the 2nd intrusion of MIP tests. Obviously, the binder with 30% FA (PF5) or 70% BFS (PB5) shows a finer PSD than that of the reference OPC binder (P5). It is not easy to differentiate the pore size fineness between the binders P5 and PFL5 directly from their PSD curves. The average pore diameter d_a, as defined by Eq. (1) to indicate the fineness of pore size, was further determined for these binders. An ascending order of the d_a is found: PB5 (d_a=11.6 nm) < PF5 (d_a=19.7 nm) < P5 (d_a=24.5 nm) < PFL5 (d_a=25.7 nm).

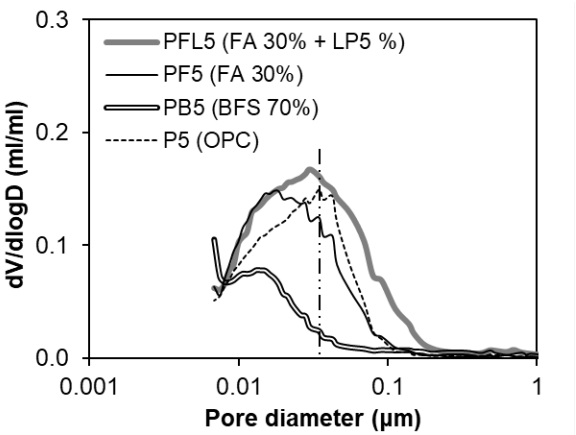

Fig. 6. Pore size distribution obtained from the 2nd intrusion of MIP tests performed on paste specimens made with different binders (one-year-old, w/b=0.5)

From the pore size effect on water continuity η_w as analyzed earlier in this paper, it is expected that for different binders the water continuity at high water saturation levels tends to present an ascending order as: η_w(PB5) < η_w(PF5) < η_w(P5) < η_w(PFL5).

4.2 Pore Connectivity

Based on the MIP tests, and using Eq. (2), the pore connectivity η_p of different paste specimens was determined. It is found that compared to the reference OPC binder P5, the binders with 30% FA or 70% BFS normally exhibit lower pore connectivity η_p. This can be ascribed to the occurrence of pozzolanic reactions that result in a higher packing density of hydrates and more tortuous pore network. To be specific, the pore connectivity η_p of different binders presents an ascending order as: PB5 (η_p=37.3%) < PF5 (η_p=45.8%) < PFL5 (η_p=55.1%) < P5 (η_p=57.1%).

4.3 Relative Chloride Diffusion Coefficient

Figure 7 shows the relative chloride diffusion coefficient D_{rc} as a function of the degree of water saturation S_w in the mortars made with different binders. In general, the D_{rc}-value shows a decreasing trend with decreasing S_w level, regardless of the binders. On the other hand, the D_{rc}-S_w relation exhibits significant differences for the different binders.

- At high saturation levels (i.e. $S_w \geq 60\%$), the D_{rc}-value shows an ascending order in the binders PB5, PF5, P5, and PFL5. Such ascending order is attributable to the same ascending order of the average pore diameter in these binders, as already obtained from Fig. 6.
- At low saturation levels (i.e. $S_w < 60\%$), the D_{rc}-value shows an ascending order in the binders PB5, PF5, PFL5, and P5. This is consistent with the same ascending order of the pore connectivity in these binders.

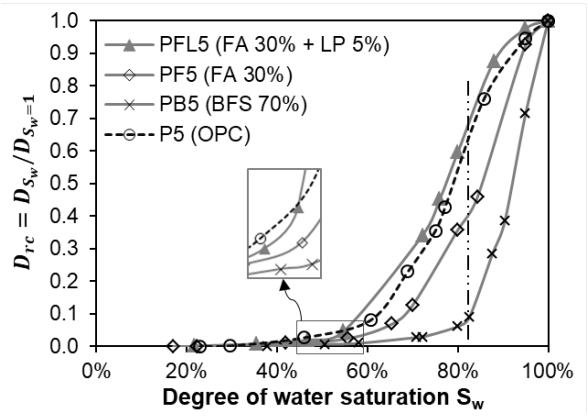

Fig. 7. D_{rc}-S_w relations for mortar specimens made with different binders (one-year-old, w/b=0.5)

The abovementioned analysis demonstrates that the D_{rc}-S_w relation is strongly dependent on the pore structure. Of interest is that compared to the binder P5, the binder PFL5 shows higher D_{rc}-values for high S_w levels while shows lower D_{rc}-values for low S_w levels.

This observation further confirms that the pore size effect on water continuity, as well as on the D_{rc}-value, is weak for low S_w levels. Instead, the pore connectivity effect plays a dominant role in the D_{rc}-value for low S_w levels.

5.0 CONCLUSIONS

The relative chloride diffusion coefficient D_{rc} at various degrees of water saturation S_w has been studied for different cementitious materials. The effects of the pore structure on the water continuity, as well as on the D_{rc}-S_w relation, were emphasized. The key findings can be drawn as follows:

- The D_{rc}-S_w relation is governed by the water continuity in the pore systems. At a particular S_w, higher water continuity results in higher D_{rc}.
- For a given pore size distribution and pore connectivity, the porosity has little influence on the water continuity and therefore does not affect the D_{rc}-S_w relation.
- A finer pore size distribution or lower pore connectivity tends to result in a lower water continuity and hence a smaller D_{rc}-value. The pore size effect on the water continuity, as well as on the D_{rc}-value, is pronounced primarily for high water saturation S_w levels. For low S_w levels, both water continuity and D_{rc}-value are dominated by the pore connectivity effect.
- For a given degree of water saturation S_w, the D_{rc} is lower in the fly ash (or slag) blended binders than in the reference OPC binders. Compared to the fly ash blended binder, further addition of limestone powder increases the D_{rc} in the entire water saturation levels tested.

Acknowledgement

Financial support from China Scholarship Council (CSC) is highly acknowledged.

References

Aligizaki, K.K., 2006. Pore Structure of Cement-Based Materials: Testing, Interpretation and Requirements. CRC Press, Taylor & Francis.

Diamond, S., 2000. Mercury porosimetry: An inappropriate method for the measurement of pore size distributions in cement-based materials. Cement and Concrete Research, 30:1517-1525.

Garboczi, E.J., 1990. Permeability, diffusivity, and microstructural parameters: A critical review. Cement and Concrete Research, 20:591-601.

Patel R.A., Phung Q.T., Seetharam S.C., Perko J., Jacques D., Maes N., De Schutter G., Ye G., Van Breugel K., 2016. Diffusivity of saturated ordinary Portland cement-based materials: A critical review of experimental and analytical modelling approaches. Cement and Concrete Research, 90:52-72.

Washburn E.W., 1921. The dynamics of capillary flow. Physical Review, 17:273-283.

Ye G., 2003. Experimental study and numerical simulation of the development of the microstructure and permeability of cementitious materials. PhD thesis, Delft University of Technology.

Zhang Y., Ye G., 2018. Influence of moisture condition on chloride diffusion in partially saturated ordinary Portland cement mortar. Materials and Structures, 51:36.